Received: 16 May 2023 | Revised: 19 October 2023 | Accepted: 6 November 2023

DOI: 10.1002/hyp.15033

RESEARCH ARTICLE

WILEY

The heat is on: Predicting urban stream temperature responses to summer storms

Julia L. A. Knapp[1] | Christa Kelleher[2]

[1]Department of Earth Sciences, Durham University, Durham, UK

[2]Civil and Environmental Engineering, Lafayette College, Easton, Pennsylvania, USA

Correspondence
Julia L. A. Knapp, Department of Earth Sciences, Durham University, Durham, UK.
Email: julia.l.knapp@durham.ac.uk

Abstract

Short-term increases in stream temperature in response to storm events have frequently been observed in urban areas, highlighting the need for improved understanding of the factors influencing urban stream temperature. Urban land cover complexity and infrastructure designed for rapid water routing to the sewer system create a direct link between storm events and water release processes, influencing urban stream temperature responses. This study aims to identify predictors of diverse stream temperature response patterns to summer storms. We analysed 403 storm events from six urban and semi-urban catchments along the US East Coast using dynamic time warping to identify archetype patterns of stream temperature responses. We further disentangled observed stream temperature increase patterns to reveal the drivers associated with 'heat pulses', which are characterized by a rapid but high-magnitude temperature increase followed by a sharp temperature drop at the start of the hydrograph increase. Our results show that stream temperature patterns were event-specific and linked to pre-event conditions and rainfall–runoff characteristics, with the shape of the hydrograph and rainfall–runoff response identified as the most important determinators of the observed temperature response patterns. Ponded surface waters and storm drains, as well as cooler water from the shallow subsurface, were identified as potential sources contributing to temperature patterns. These findings have important implications for understanding urban hydrology and the contributions of different source zones in urban catchments. Specifically, our results suggest that stream temperature may serve as a cost-effective tracer providing information about urban water sources and pathways, thus aiding in the understanding of complex urban hydrology.

KEYWORDS

heat pulse, rainfall–runoff characteristics, storm events, stream temperature, tracer, urban hydrology

1 | INTRODUCTION

Stream temperature is an important water quality parameter that plays a pivotal role in controlling metabolic and other reaction processes (Arnell, 1998) and the survival of most aquatic species. High water temperatures can increase stress for benthic organisms (Winterbottom et al., 1997) and fish populations (Gooseff et al., 2005), making it essential to maintain a suitable temperature

range. Stream temperature in urban environments may differ from stream temperature in forested and rural areas, with urban areas acting as heat sources and creating temperature discontinuities along rivers (Arora et al., 2018). The degradation of water quality and ecological status of streams draining urban areas is referred to as 'urban stream syndrome' (Walsh et al., 2015), an umbrella term that characterizes a range of responses that have been observed in urban systems. In particular, streams experiencing urban stream syndrome often drain high percentages of impervious areas, exhibit flashy hydrographs due to rapid routing of rain water to the stream, reduced biodiversity, and increased nutrient and contaminant concentrations, in addition to stream temperature changes (Nelson & Palmer, 2007).

Past studies have shown that stream temperature in urban areas depends substantially on the near-stream land cover. Riparian buffer zones may cool urban stream temperatures (Arora et al., 2018), whereas effluent from waste water treatment plants is known to raise stream temperatures (Beganskas & Toran, 2021). Furthermore, stormwater control measures can substantially influence stream temperature by impacting urban discharge (Fanelli et al., 2019) as well as the temperature of the added localized runoff (Ouellet et al., 2021; Timm et al., 2020). More recently, a positive relationship has been observed between length of stormwater pipes and daily water temperatures (Timm et al., 2021). In consequence, stream temperature is highly dependent on the specific layout of the urban system.

Stream temperature is known to fluctuate on annual, seasonal, and daily basis, however, storm events may additionally impact stream temperature on even shorter time scales. In particular, short-term increases in stream temperature in response to storm events have frequently been observed in urban areas. In the Maryland piedmont, Nelson and Palmer (2007) measured temperature increases associated with storms of up to 7°C, mostly at urbanized sites. Similarly, Somers et al. (2013) documented increases of around 4°C during storms in urban catchments, but only insignificant temperature changes at forested sites. More recently, Beganskas and Toran (2021) found that the frequency and magnitude of stream temperature increases correlated well with the percentage of impervious land cover at the watershed scale. At regional scales, Zahn et al. (2021) documented the highest frequency of temperature increases in highly developed watersheds with a low percentage of vegetated area.

While many studies have sought to quantify stream temperature responses, it has also been noted that temperature increases do not occur during every summer storm. For example, Beganskas and Toran (2021) only observed temperature increases during 6%–32% of days with rain, and found no difference in regional precipitation characteristics between days with and without temperature changes. Consequently, temperature increases may occur during some events but not others at the same site. Similarly, the shape and form of these stream temperature responses may vary, and (gradual) temperature increases do not appear to be the only possible stream temperature response during a storm event. Zahn et al. (2021) observed that temperature increases may be followed by a subsequent rapid decrease in water temperature, a pattern we will refer to as a 'heat pulse' in our study. However, further exploration of this phenomena has been limited. Altogether, this indicates that stream temperature responses associated with storm events may be more diverse than has been previously thought, with respect to magnitude, direction, and timing of their response. Of the few studies that explore stream temperature increases at city to regional scales, the majority focus on extracting a handful of stream temperature metrics from each storm, most often the total magnitude of temperature change (and even more commonly limited to positive changes) over the course of the storm event. These, however, are not able to capture the complexity of water temperature responses to storm events, which may represent a missed opportunity to assess water release processes from storm responses.

In this study, we aim to understand event-specific predictors of diverse stream temperature responses to summer storms. For this purpose, we analyse stream temperature, discharge, and precipitation data from six urban and semi-urban catchments located at the East Coast of the US during storm events of three consecutive summers. We assess variations in stream temperature responses associated with storm events, and link the response types to storm event characteristics. We also examine 'heat pulses' more closely, that is, brief but substantial increases in stream temperature at the beginning of an event followed by a rapid drop in stream temperature, to understand which event characteristics influence the occurrence and magnitude of these pulses. We hypothesize that a combination of time-varying factors related to precipitation intensity, streamflow response, time of day, and seasonality (e.g., time of year) will ultimately organize stream temperature responses across events and create distinct stream temperature patterns as function of event characteristics.

2 | STUDY AREA

We focus on data from six semi-urban and urban watersheds located on the US East Coast. The sites were chosen because each gaging station was located within 15 miles of a high resolution precipitation station. All sites are located in semi-urban to urban areas with moderate to high percentages of impervious area (Table 1, Figure S8); notably, sites were not selected to span a land cover gradient, and the effect of land cover is not evaluated in our analysis. According to the HydroWASTE dataset (Ehalt MacEdo et al., 2022), none of the watersheds contain wastewater treatment plants.

Geographically, sites cluster within two general areas: the Philadelphia-Baltimore-Washington DC area, and the metropolitan Atlanta area. We briefly summarize key aspects of each site below, ordered from North to South. Site figures are included in the supplementary material.

Cobbs Creek (Figure S1) drains a semi-urban catchment northwest of Philadelphia, Pennsylvania with large areas of imperviousness. The immediate riverbanks are forested. Average discharge during the years 2015–2020 was 0.21 m^3/s.

Carroll Creek (Figure S2), located in Frederick, Maryland, drains forested hills in its headwaters with semi-urban industrial and residential areas and significant areas of open grassland closer to the gauge. A narrow buffer strip protects the immediate stream, and average discharge of the years 2018–2020 was 0.46 m^3/s.

TABLE 1 List of streamwater sites used in this study, including their USGS Site numbers and catchment areas, and some measures of land use.

Site name	State	USGS Site reference	Catchment area (mi^2)	Forested area (%)	Developed area (%)	Impervious area (%)
Cobbs Creek at US Highway No. 1	PA	01475530	4.78	8.2	91.0	29.0
Carroll Creek above Rock Creek	MD	01642199	7.33	24.6	50.3	17.7
Hickey Run at National Arboretum	DC	01651770	1.01	1.5	97.7	60.6
Little Stone Mountain Creek near Stone Mountain	GA	02207135	2.20	38.7	60.2	11.4
Woodall Creek at Defoors Ferry Road	GA	02336313	2.71	7.6	90.8	59.1
Doolittle Creek at Flat Shoals Road	GA	02203831	4.25	15.3	83.2	21.7

Note: Catchment area information is taken from the USGS National Water Information System. Watersheds were delineated in StreamStats, and used to extract information on the 2021 percentage of forested area, developed land cover and percent developed imperviousness (Dewitz, 2023).

Hickey Run (Figure S3) is located in north eastern Washington DC, within the National Arboretum. Large parts of the catchment are now underground, confined to artificial storm pipes, and only a short section of the stream remains in its natural state. The impervious area of the watershed has increased substantially in the past 30 years (DOE, 2022). Average discharge was 0.06 m^3/s during the years 2015–2020.

Little Stone Mountain Creek (Figure S4) is a small headwater stream in a semi-urban catchment in Dekalb County, Georgia, northeast of Atlanta. The watershed lies mostly in a residential area with large amounts of forest cover, particularly along the stream banks. Average discharge was 0.21 m^3/s during the years 2015–2020.

Woodall Creek (Figure S5) is a headwater stream located in northern Atlanta, Georgia. The watershed is forested close to the gauging station, but drains an industrial area further upstream with large impervious surface coverage. The stream banks are forested along most of its length, though the extent of this buffer strip is narrow in most places. Average discharge was 0.13 m^3/s during the years 2015–2020.

Doolittle Creek (Figure S6) is a semi-urban catchment in the East of Atlanta, Georgia. It drains a residential area with some forested areas along the riverbanks, and larger areas of grassland throughout the watershed. At its source, Doolittle Creek drains a small lake belonging to a golf club. Average discharge was 0.43 m^3/s during the years 2015–2020.

3 | METHODS

3.1 | Dataset

Discharge, precipitation, and stream temperature data were obtained from the USGS National Water Information System for the years 2019–2021. Winter data were either minimally or not available at some of the sites due to snow cover and ice. For this reason, we restricted our analysis to the periods of 1st May until 30th September for the years 2019, 2020, and 2021 at all six sites. At most sites, discharge and stream temperature data were available at 15 min intervals, except at Hickey Run (2 min) and Carroll Creek (5 min). The temporal resolution of the precipitation data normally matched the resolution of the discharge data, except at Hickey Run, where precipitation information was provided at 5 min intervals.

To determine watershed land use and cover, we first delineated each watershed to the latitude and longitude of the USGS monitoring location using StreamStats (https://streamstats.usgs.gov/ss/). We then extracted the percentage of forest cover (classes 41–43, including deciduous, evergreen and mixed forest) and the percentage of developed land cover (sum of classes 21–24) from the 2021 National Land Cover Database (NLCD) Land Cover dataset and imperviousness from the 2021 NLCD Percent Developed Imperviousness dataset (Dewitz, 2023) with a grid resolution of 30 m. This information was extracted for each watershed in ArcMap (v. 10.8.2) and the values are reported in Table 1.

3.2 | Data analysis

3.2.1 | Event identification

Hydrologic events were identified using the MATLAB package HydRun (Tang & Carey, 2017). In this, an event was classified as an increase in discharge of at least the mean discharge value of the time series. Events were cut at 60% recession, but events with shorter recession were also included in the analysis, as long as three or more data points for both discharge and stream temperature were available after the discharge peak. This threshold is somewhat arbitrary but was selected to enable identification of a large range of event sizes. Events without stream temperature data were excluded from further analysis. In total, this resulted in 677 analysable events across all sites and years.

3.2.2 | Identification of temperature patterns

We identified different stream temperature patterns and assessed their relative frequency at each site based on the 677 events with

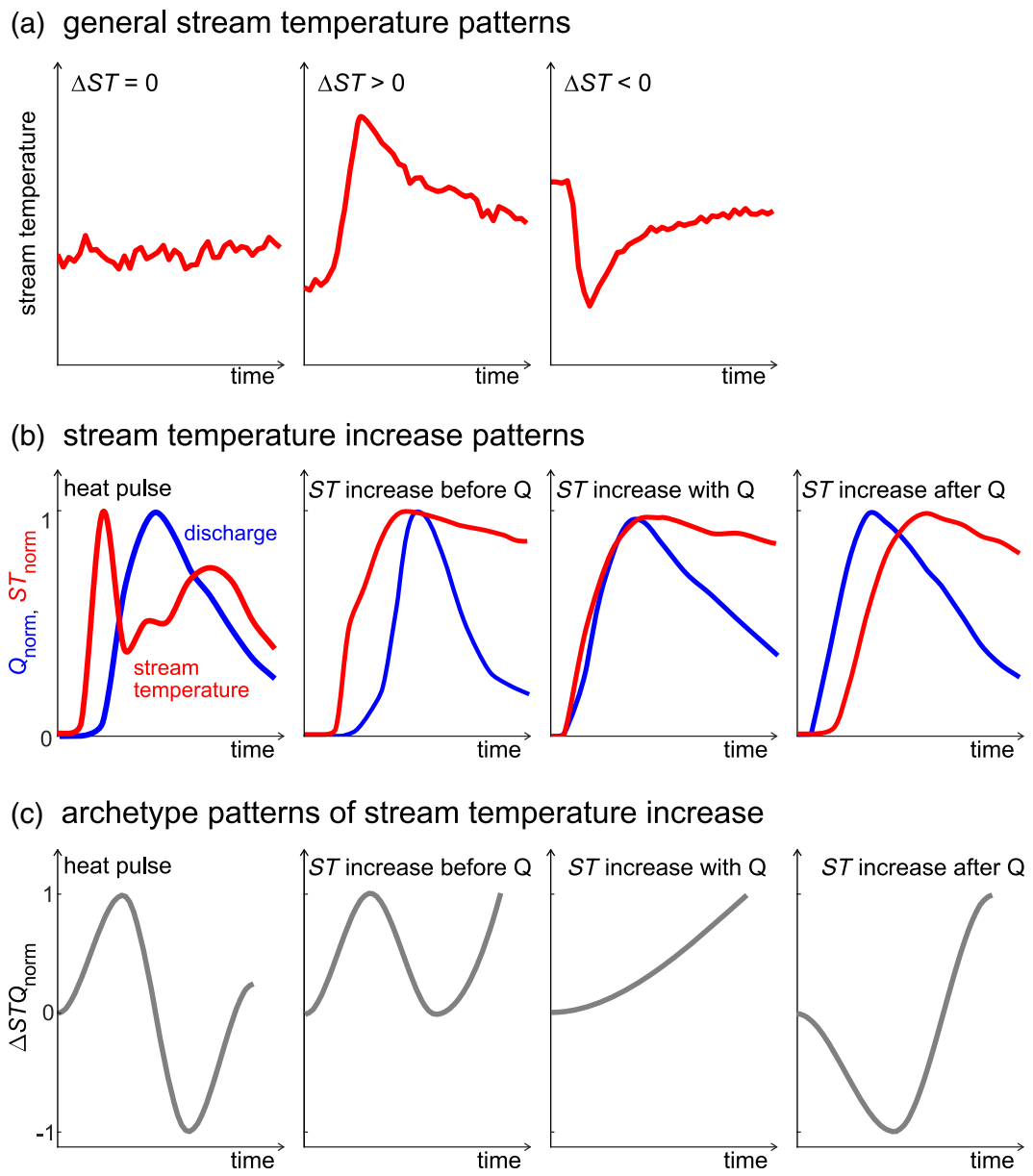

FIGURE 1 (a) General stream temperature patterns: no change in stream temperature ($\Delta ST = 0$), increase in stream temperature ($\Delta ST > 0$), and decrease in stream temperature ($\Delta ST < 0$). These are identified based on stream temperature alone. (b) Scaled stream temperature and discharge of the different stream temperature increase patterns: heat pulse, stream temperature increase before discharge, stream temperature increase with discharge, and stream temperature increase after discharge. (c) Archetype cluster patterns related to the *ST* increase patterns shown in (b).

stream temperature data. This comparison aimed to identify whether sites were more likely to exhibit one dominant pattern, or whether a wider range of patterns occurred at the different sites. Comparing across 3 years also allowed us to test the stability of the different patterns over time. For this analysis, we classified general response patterns in a first step, and further disentangled temperature increase patterns in a second step.

General stream temperature patterns

First, we classified the general temperature response patterns of stream temperature (increase, decrease, or no change) during each event (Figure 1a). Events where the average temperature change during the event was smaller than 0.25°C/h were classified as '*no stream temperature change*' ($\Delta ST = 0$). A *stream temperature increase* ($\Delta ST > 0$) was diagnosed if the difference between the maximum temperature and the pre-event baseflow temperature was at least twice as large as the difference between the minimum temperature and the pre-event temperature. Similarly, a *stream temperature decrease* ($\Delta ST < 0$) was identified if the difference between pre-event temperature and minimum temperature was at least twice as high as the difference between maximum temperature and the pre-event temperature:

$$\Delta ST = 0 \text{ if } \frac{ST_{max} - ST_0}{t_{event}} < 0.25^{\circ}\text{C/h}, \quad (1)$$

$$\Delta ST > 0 \text{ if } ST_{max} - ST_0 > 2 \cdot (ST_0 - ST_{min}), \quad (2)$$

$$\Delta ST < 0 \text{ if } ST_0 - ST_{min} > 2 \cdot (ST_{max} - ST_0), \quad (3)$$

with the minimum and maximum temperature during the event, ST_{min} and ST_{max}, the pre-event stream temperature measured directly before the start of the event, ST_0, and the duration of the event, t_{event}. Any temperature change falling between the two end members of temperature increase and decrease was classified as an unclear pattern and not included in the analysis.

Stream temperature increase patterns

Next, we identified and separated various types of temperature increases, including events with a rapid, short temperature increase followed by a rapid drop in temperature at the start of the event (a pattern we will refer to as 'heat pulse' in the following). Visual inspection of the events featuring an increase in stream temperature revealed four different archetype patterns of the timing in temperature increases relative to the timing of the hydrograph (Figure 1b):

1. a heat pulse, that is, a rapid temperature increase occurring at the very start of the discharge rise, followed by a rapid drop in stream temperature;
2. an increase in stream temperature before the rise of the hydrograph, with stream temperature continuing to stay high until at least the hydrograph peak;
3. an increase in stream temperature at approximately the same time as the rise of the hydrograph;
4. an increase in stream temperature delayed relative to the rise of the hydrograph, that recedes very slowly.

To identify these patterns in a systematic way, we classified the timing of the stream temperature change relative to the timing of the discharge rise. This required scaling both temperature and discharge to a range from 0 (discharge Q_0 and stream temperature ST_0 during pre-event baseflow) to 1 (maximum values of discharge, Q_{max}, and stream temperature, ST_{max}):

$$Q_{norm}(t) = \frac{Q(t) - Q_0}{Q_{max} - Q_0}, \quad (4)$$

$$ST_{norm}(t) = \frac{ST(t) - ST_0}{ST_{max} - ST_0}. \quad (5)$$

Finally, we calculated the difference of ST_{norm} and Q_{norm} and scaled it again to yield ΔSTQ_{norm}:

$$\Delta STQ(t) = ST_{norm}(t) - Q_{norm}(t), \quad (6)$$

$$\Delta STQ_{norm}(t) = \begin{cases} \frac{\Delta STQ(t) - \Delta STQ_0}{\Delta STQ_{max} - \Delta STQ_0} & \text{if } \Delta STQ_{max} > |\Delta STQ_{min}| \\ \frac{\Delta STQ(t) - \Delta STQ_0}{\Delta STQ_0 - \Delta STQ_{min}} & \text{else} \end{cases}. \quad (7)$$

The repeated scaling is necessary to ensure comparability between small and big events (Equation 4), events with higher and lower average temperatures and temperature changes (Equation 5), and events with stronger and weaker ratios of temperature and discharge changes (Equation 7). It thus allows comparing events based on the relative timing of discharge and temperature, rather than the magnitudes of discharge and temperature.

To identify the most representative stream temperature pattern for each event, we created archetypes of the four clustering patterns quantifying the difference between normalized discharge and normalized stream temperature (Figure 1c) and performed dynamic time warping between ΔSTQ_{norm} and the four archetype patterns of temperature increase. Dynamic time warping quantifies the smallest Euclidian distance between signals with variable timing, by stretching and compressing the signals to find the closest match between them. We then used the calculated Euclidian distance between the 'warped' signals to assess the goodness of fit of ΔSTQ_{norm} to the four archetype patterns. To account for the different shapes and ranges of the archetypes, we subtracted the distance value obtained from dynamic time warping of the archetype and its mean value from the distance between the time series and the archetypes. The archetype pattern that fitted the ΔSTQ_{norm} pattern the best (i.e., resulted in the smallest Euclidean distance) was selected as the most representative temperature increase pattern. The analysis was performed in MATLAB R2020b using the function `dtw` (Paliwal et al., 1982; Sakoe & Chiba, 1978) of the Signal Processing Toolbox. A visual inspection was additionally performed to confirm the identified archetype pattern for each event.

3.2.3 | Heat pulse magnitudes and mixing analysis

Finally, we calculated the magnitudes of the temperature increase for those events featuring a heat pulse. This heat pulse magnitude was quantified as the largest temperature increase within 15 min occurring at any time throughout the event. An interval of 15 min (14 min at Hickey Run) was selected because the temperature increases of most heat pulses lasted for approximately 15–30 min. We confirmed that the magnitude of the 15 min temperature rise was not significantly biased by the temporal resolution of the data set, by comparing the calculated magnitudes of 15 min temperature changes at Hickey Run and Carroll Creek at the supplied temporal resolution (2 and 5 min, respectively) and for subsampled datasets at both sites. Our analysis showed that aggregating to 15 min only resulted in a very small underestimation of the heat pulse magnitude (less than 10%, Figure S7). To identify the potential sources of the water contributions resulting in heat pulses, we additionally quantified the water

TABLE 2 A list of predictor (explanatory) variables assessed in the bootstrap forest model and the logistic regression analyses.

Metric	Unit	Description
Antecedent conditions and event timing:		
date	(day)	Julian Date—Day of year since 01-Jan
ToD	(h)	Time of day since midnight
T_0	(°C)	Stream temperature at baseflow before the hydrograph rise
P4d	(mm)	Antecedent wetness as the total volume of precipitation fallen in the 4 days prior to the storm event
Q_0	(mm/d)	Discharge before the start of the hydrograph increase
Hydrograph metrics:		
t_{rise}	(h)	Time of rise—time between start and peak of hydrograph
Q_{peak}	(−)	Discharge value at peak, normalized by the mean discharge of the time series
ΔQ	(mm/d)	Discharge increase between baseflow and peak flow
Q_{peak}/V_Q	(1/d)	Peak discharge value related to total runoff, this assesses the shape of the hydrograph, with larger values indicating shorter relative events.
Rainfall and input metrics:		
t_{rain}	(d)	Rainfall duration
I_p	(mm/d)	Rainfall intensity
C	(−)	Runoff coefficient
$t_{response}$[a]	(h)	Time between start of rain event and hydrograph increase
$t_{centroid}$[a]	(h)	Time between centroid of rain event and centroid of hydrograph

Note: The predictor include a range of different characteristics of the pre-event characteristics, the hydrograph, and the precipitation input, all hypothesized to be related, either directly or indirectly, to stream temperature responses to storm events.
[a]Both metrics quantify lag times between rain and runoff, however, they are only weakly correlated describing very different aspects of the lag, which justifies including both as potential predictor variables.

temperature of added runoff required to raise stream temperatures at a given site by our quantified heat pulse magnitudes. For this purpose, we performed a simple mixing analysis, explained further in Supporting Information S6.

3.2.4 | Relationship of water temperature patterns to predictor variables

We assessed the influence of event characteristics on the different temperature patterns using a bootstrap forest model and logistic regression analysis. Both analyses were performed in JMP Pro 16. In both analyses we assessed predictor variables describing a wide range of storm event characteristics, metrics of the precipitation input and its discharge response as well as the pre-event conditions (Table 2). These predictors were selected because they are hypothesized to either directly or indirectly capture the routing and response of urban rainfall–runoff processes. The relationship between the different predictor variables was additionally assessed through the calculation of Spearman's rank correlation coefficients.

Because the predictors also include characteristics of the rain events, we excluded from the analyses all events for which no precipitation data were recorded or for which the identified precipitation event incorrectly appeared to start after the first rise of the hydrograph ($n = 268$). This can happen if the precipitation event is highly localized and occurs away from the rain gauge. We also excluded an additional six events during which the calculated rainfall–runoff coefficient was greater than 1, indicating possible complications with the rainfall data. In total, this resulted in the exclusion of 274 events from the analysis, meaning 403 storm events remained for the bootstrap forest and logistic regression analyses. The exclusion was not biased toward specific types of events, as we excluded 70 out of 222 events without temperature change (32%), 166 out of 362 events with a temperature increase (46%), and 38 out of 93 events with a temperature decrease (41%).

The bootstrap forest analysis is a type of predictor screening that can be used to assess many different variables for their ability to predict an outcome (Hastie et al., 2009), and thus provides insights into the variables relevant for stream temperature patterns as a whole. The bootstrap forest method estimates a response by averaging predictions from multiple decision trees. Each tree is developed using a bootstrap sample from the training data, which is a random selection of observations with replacement. Here, the bootstrap forest model was constructed using 100 decision trees for each response variable to evaluate the relative contribution of each predictor to the response. Response variables in this analysis were the two categorical temperature patterns (general stream temperature change, and the temperature increase pattern), and also the heat pulse magnitude.

A logistic regression analysis is similar to a linear regression analysis, but applies to categorical rather than continuous response variables. It can be used to model the relationship between explanatory (or predictor) and response variables and assesses the probability of different outcomes (in this case, the identified temperature patterns) as a function of the explanatory variables. Parameter estimates determined for the different explanatory variables provide information on the characteristics deciding the type of stream temperature response. It thus allows dissecting the relationship between individual stream temperature patterns and predictor variables in more detail. Here we used a stepwise approach to generate the output model, which successively excluded predictors with the highest p-value, that is, the lowest predictive power, until the model only included predictor variables with p-values <0.05. Separate logistic regression analyses were run for the general stream temperature patterns and the temperature increase patterns.

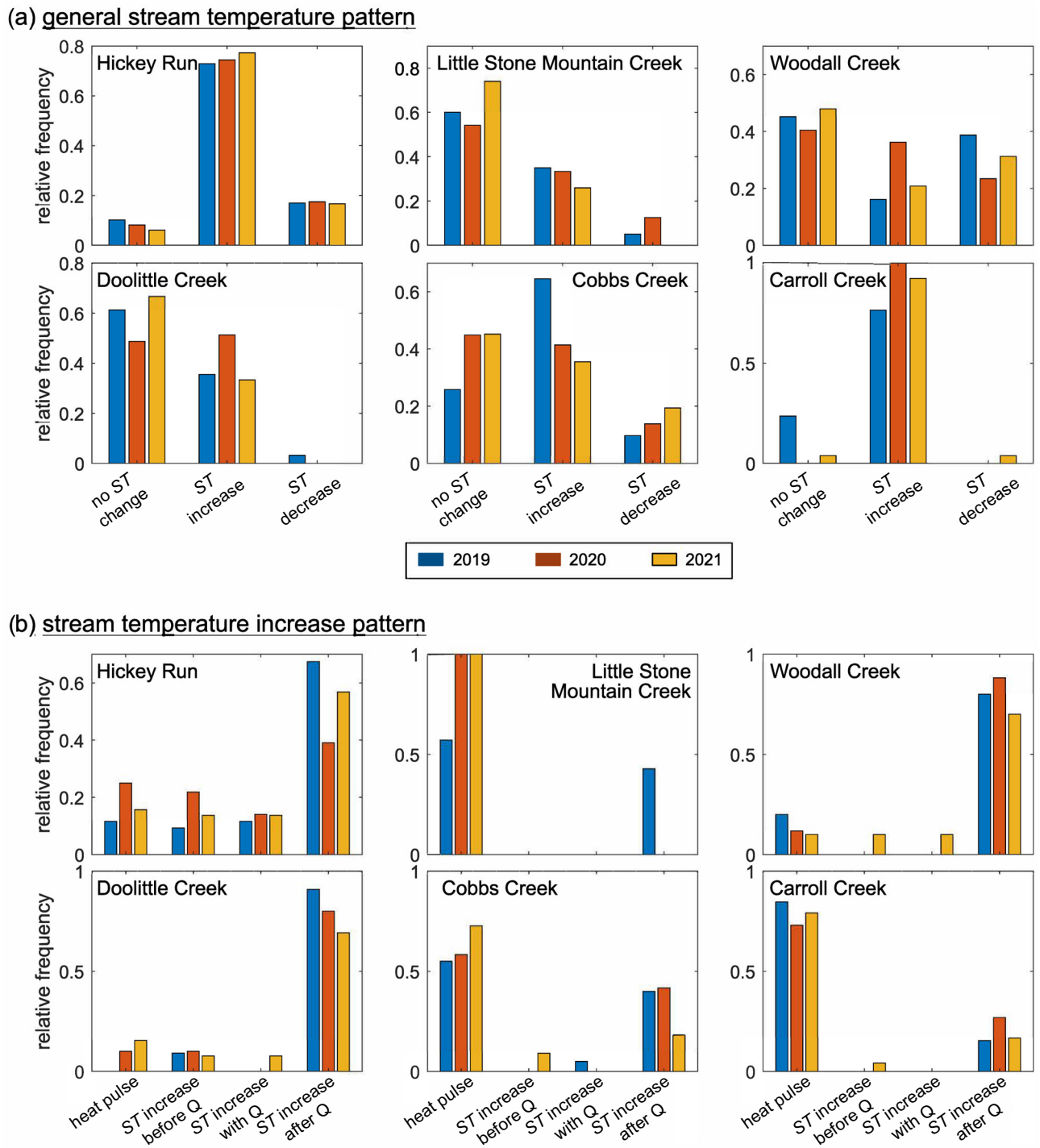

FIGURE 2 (a) Relative frequency of general stream temperature response patterns to storm events across the years 2019 (blue), 2020 (red), and 2021 (yellow). Responses vary greatly across sites but are relatively consistent over time. (b) Relative frequencies of different temperature increase patterns. Heat pulses and stream temperature increases after discharge seem to be the most typical increase responses, and these patterns are highly site-specific.

4 | RESULTS

4.1 | Stability of general temperature patterns and temperature increase patterns

Across all sites and years, stream temperature did not change during 33% of events ($\Delta ST = 0$), increased during 53% of events ($\Delta ST > 0$), and decreased during 14% of events ($\Delta ST < 0$). The observed patterns were mostly stable over the 3 years, with the relative frequencies of the general temperature response patterns similar in the summers of 2019, 2020, and 2021 at each site (Figure 2a). This was especially true for sites with one dominant pattern (e.g., Hickey Run and Carroll Creek), whereas sites with a greater variety of patterns also exhibited greater variability across the years (e.g., Little Stone Mountain Creek, Cobbs Creek).

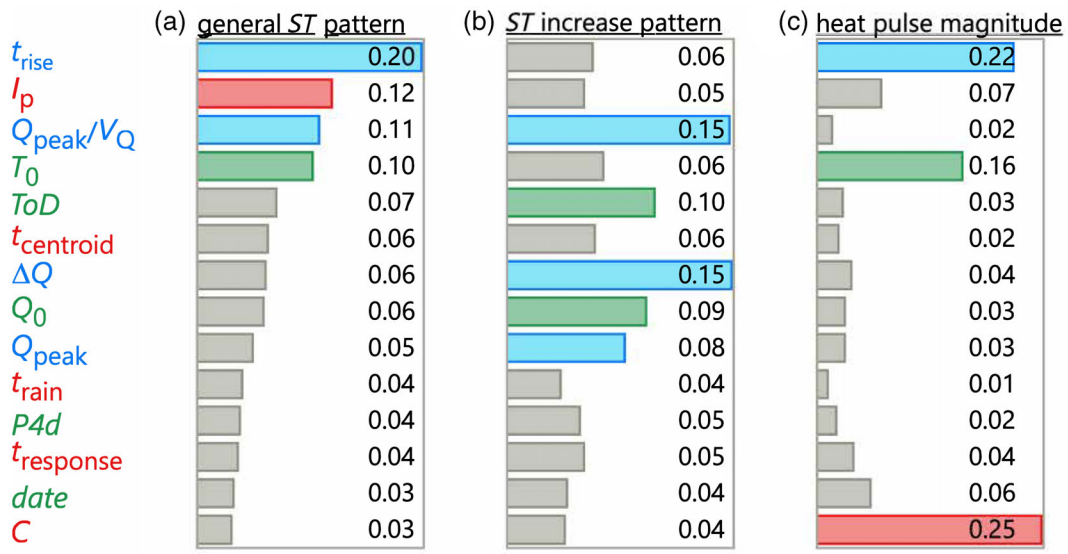

FIGURE 3 Results of the bootstrap forest analysis. The bars quantify the relative contribution of each predictor variable to the bootstrap forest model for the general stream temperature change pattern (a; no T change, *ST* increase, and *ST* decrease), the temperature increase pattern (b; heat pulse, gradual *ST* increase), and for the heat pulse magnitude (c). The most important predictors, which contribute jointly at least 50% to the overall outcome, are coloured, and the colouring corresponds to the type of characteristic described in Table 2 (green: antecedent conditions and event timing; blue: hydrograph metrics; red: precipitation input metrics).

We used dynamic time warping to further subset the different stream temperature increase patterns. Most temperature increase patterns consisted of either heat pulses (in 36% of all events with a temperature increase) or a delayed increase in temperature relative to the hydrograph (in 48% of all events with a temperature increase). An increase in water temperature slightly before or at the same time as the hydrograph rise occurred in only 15% of all events. For all further pattern-based analyses of the temperature increase patterns (i.e., the bootstrap forest and logistic regression analyses), we thus compared the events with heat pulses to a lumped category of the other temperature increase patterns featuring a more gradual response (*ST* increase before, with and after *Q*).

The water temperature increase patterns were mostly site specific. Heat pulses were the dominant response at Little Stone Mountain Creek, Cobbs Creek, and Carroll Creek, whereas temperature typically increased with a delay to the hydrograph at Hickey Run, Woodall Creek, and Doolittle Creek (Figure 2b). Heat pulse magnitudes varied from 0.2 to 6.8°C.

No relationship between the relative number of events with stream temperature increases and the frequency of heat pulses was observed. At both Hickey Run and Carroll Creek, the most frequent general temperature pattern was a water temperature increase. But at Hickey Run, nearly all of these were temperature increases after the hydrograph increase, whereas the events at Carroll Creek typically featured a heat pulse at the start of the event. Hence it does not appear that a specific general stream temperature patterns (no *ST* change/*ST* increase/*ST* decrease) makes a specific temperature increase pattern (gradual or heat pulse) more likely.

4.2 | Bootstrap forest analysis

The bootstrap analysis identified a range of characteristics related to the hydrograph, precipitation, and the pre-event conditions as the most relevant predictor variables for the general stream temperature pattern (Figure 3a). In particular the time of rise (t_{rise}), the shape of the hydrograph (Q_{peak}/V_Q), the precipitation intensity (I_p), and the pre-event baseflow temperature (T_0) were identified as important predictors. We note that some of these predictor variables are correlated (Table S3), with a faster hydrograph increase (shorter t_{rise}) typically coinciding with higher precipitation intensities and narrower hydrographs (higher Q_{peak}/V_Q and I_p values). A higher pre-event baseflow temperature (T_0) is also related to stronger precipitation intensities (I_p). These correlations are not always strong, but in all cases statistically significant. While these significant but weak to moderate correlations exist among these predictors, we have not excluded these predictors, as we are interested in a first order assessment of the key empirical predictors of water temperature storm responses.

Hydrograph characteristics were the most important predictors for distinguishing the stream temperature increase pattern (i.e., distinguishing between heat pulses and more gradual stream temperature increase patterns, Figure 3b). In particular the shape of the hydrograph (Q_{peak}/V_Q), the discharge change (ΔQ) and peak discharge (Q_{peak}) played an important role. Additionally, metrics of antecedent conditions (the pre-event baseflow value, Q_0) and the event timing (the time of day, *ToD*) played a role in determining the temperature increase pattern.

Conversely, the types of predictors relevant for the heat pulse magnitude (Figure 3c) were related to a mix of predictor variables,

including the runoff coefficient (C), the time of rise of the hydrograph (t_{rise}), and the pre-event stream temperature (T_0). The largest temperature increases were observed for low runoff coefficients and fast discharge increases (Figure S9a,b). However, this part of the analysis should be treated with caution, given that the dataset only includes 71 events with heat pulses. Although bootstrap forest is a robust algorithm that can handle small samples, it is typically recommended that the dataset is about 10 times the number of variables, which is not the case for the heat pulse analysis.

In consequence, the predictors influencing the type of response (Figure 3a,b) differed from those most important for the magnitude of the heat pulse response (Figure 3c). For example, how fast the hydrograph increases (i.e., the time between first increase in discharge and the discharge peak, t_{rise}) was highly relevant for the general temperature pattern and the heat pulse magnitude, but much less important for the temperature increase pattern. One can also identify predictor variables that appear to be of little relevance in this study. These are largely related to antecedent conditions (like *P4D*), the event itself (e.g., *date*, although it should be noted that only events during the months from May to September were assessed here) and rainfall–runoff metrics (lag times like $t_{centroid}$ and $t_{response}$).

It should be noted that a bootstrap forest analysis can identify the most important predictors influencing different response variables. It, however, does not make any statements regarding the direction of the relationship between the predictor and response variables, merely identifying the dominant influencing variables.

4.3 | Logistic regression analysis

The logistic regression analyses were able to correctly identify the general stream temperature patterns of 306 out of 403 events (76%), and the correct temperature increase pattern in 144 out of 196 events (73%). The relative amount of correctly identified events for each type of event ranged from 15% to 86%. Stream temperature decrease patterns had the lowest probability of correct identification at 15%, likely due to the generally small number of events featuring this pattern. Thus, relationships to event characteristics identified for this particular temperature pattern should be treated with caution. Conversely, all other patterns were correctly identified with a probability of at least 52% (Table S1).

The model predicting the general stream temperature change included nine explanatory variables with p-values <0.05 describing a wide range of characteristics, including aspects of the hydrograph (t_{rise}, ΔQ and Q_{peak}/V_Q), precipitation event (I_p, $t_{response}$), and timing and antecedent conditions (T_0, Q_0, *date*, and *ToD*). Only six explanatory variables were required for the model distinguishing between different patterns of temperature increase (Table 3), which were largely related to the hydrograph (Q_{peak}/V_Q, ΔQ) and antecedent and timing characteristics (T_0, Q_0, *date*, and *ToD*).

The results of the logistic regression analyses illustrate the influence of different event characteristics on the general temperature responses and temperature increase patterns (Figure 4). Events without a stream temperature change were characterized by slow and smaller increases in the hydrograph (long t_{rise}, small ΔQ) after low-intensity storms (small I_p). This suggests that watershed sources were contributing more slowly to streamflow, and likely stemming from further upstream, with such a type of response only marginally changing the stream temperature during the storm event. Conversely, events with a decrease in stream temperature were more likely to occur when the baseflow temperature was already substantially elevated (high T_0), for example, on warmer days. These events showed a large, but slower and less flashy responses (higher $t_{response}$). Consequently, a higher pre-event temperature of the streamwater (T_0), and a longer lag time between the precipitation event and streamflow response ($t_{response}$) increased the likelihood of a temperature decrease. Finally, events with temperature increases typically featured narrow, peaked, and fast-rising hydrographs (high Q_{peak}/V_Q, short t_{rise}) with substantial changes in runoff and starting at low baseflow values (high ΔQ, small Q_0) following high-intensity precipitation (high I_p). Often, these events occurred in the late afternoon, evening and during the night. The rank correlation analysis (Table S3) revealed only a weak correlation between the time of day and precipitation intensity, meaning that intense thunderstorms in the later hours of the day are not a key correlate for the observed increases in water temperature.

Disentangling events with a temperature increase further, we identified hydrograph metrics as particularly relevant (Figure 4b). A heat pulse was most likely if the runoff change (ΔQ) was high, but the hydrograph was broad (small Q_{peak}/V_Q), and the pre-event water temperature was low (small T_{ini}). Heat pulses were also more likely in the afternoon of late summer days (high *date* and *ToD*).

In logistic regression analyses, the parameter values quantify the effect of a one-unit change in the explanatory variable. However, the absolute parameter values should not be compared among each other, because the different explanatory variables have variable ranges (e.g., $0 \le C \le 1$, $11.8°C \le T_0 \le 30.3°C$, whereas $0\ mm \le P4d \le 150\ mm$ in this dataset). Instead, their statistical significance provides a useful measure of their importance. (Comparability of parameter values is possible through standardization of parameter ranges before the analysis, the results of which are shown in Table S2.)

5 | DISCUSSION

Stream temperature changes associated with storm events are diverse, both in their timing relative to streamflow, and in regard to the shape these temperature changes take. Importantly, stream temperature responses to storm events are not limited to gradual temperature increases, but may take different shapes. These may differ from event to event, and can consist of a rapid, short temperature increase and drop at the start of the hydrograph (i.e., a 'heat pulse'), or take the shape of a more gradual temperature increase or decrease.

The importance and direction of the different event characteristics in predicting the various stream temperature patterns is schematically illustrated in Figure 4. The most important predictors for the

TABLE 3 Results of the logistic regression analysis for (a) the general stream temperature pattern, and (b) the temperature increase pattern intended to aid the interpretation of Figure 4.

(a) General stream temperature pattern				(b) Stream temperature increase pattern	
	No *ST* change ↔ *ST* decrease	No *ST* change ↔ *ST* increase	*ST* increase ↔ *ST* decrease		Heat pulse ↔ gradual increase pattern
t_{rise}	0.69 ± 0.18*	0.87 ± 0.16*	−0.19 ± 0.17	Q_{peak}/V_Q	−0.05 ± 0.01*
T_0	−0.23 ± 0.09*	0.17 ± 0.06*	−0.41 ± 0.08*	T_0	−0.31 ± 0.08*
I_p	−0.16 ± 0.06*	−0.20 ± 0.06*	0.04 ± 0.04	ΔQ	0.00 ± 0.00*
ΔQ	−0.01 ± 0.00*	−0.01 ± 0.00*	0.00 ± 0.00	*date*	0.02 ± 0.01*
$t_{response}$	−0.14 ± 0.06	0.04 ± 0.05	−0.18 ± 0.05*	*ToD*	0.07 ± 0.03*
date	0.02 ± 0.01*	0.01 ± 0.00	0.01 ± 0.01*	Q_0	0.19 ± 0.10
ToD	−0.05 ± 0.03	−0.07 ± 0.02*	0.01 ± 0.03		
Q_0	0.10 ± 0.09	0.21 ± 0.10*	−0.11 ± 0.08		
Q_{peak}/V_Q	−0.03 ± 0.01	−0.03 ± 0.01*	0.01 ± 0.01		

Note: The analysis compares two categories in each column, and the parameter estimate indicates the increased probability of a certain outcome with changing explanatory value. For example, the parameter estimate of 0.69 for t_{rise} in the first column indicates that the 'no *ST* change' pattern becomes more likely compared to the '*ST* decrease' pattern if t_{rise} increases. In logistic regression without standardized parameter values, the parameter values quantify the effect of a one-unit change in the explanatory variable; in consequence, their statistical significance (variables with *p*-value <0.05 are indicated by an asterisk) can be used to assess their relative importance. Comparability of regression values is possible through standardization of the parameter ranges before the analysis, the results of which are shown in Table S2.

general stream temperature response patterns were related to the shape of the hydrograph (e.g., with a slow rise and small increase in discharge most likely not resulting in a temperature change) and to the rainfall and input metrics (e.g., with stronger precipitation intensities favouring a temperature increase). Conversely, a high pre-event stream temperature and a long response time between precipitation input and hydrograph response was related to a temperature decrease.

The day of year and time of day were also linked to the type of temperature response. Events with temperature increases were more likely to occur in the afternoon/evening, whereas stream temperature decreases typically occurred earlier in the year (before the middle of July, day of year 200). The finding that time of day is linked to the occurrence of temperature increases is in agreement with work by Zahn et al. (2021), who quantified heat pulses across 100 watersheds in the midwestern and eastern US, and Hester and Bauman (2013), who observed water temperatures near urban storm sewer outfalls in Virginia, USA. Both studies observed a greater frequency and magnitude of temperature increases in the afternoon when pre-event discharge and pre-event temperatures were higher. These two variables were significantly related to both *date* and *ToD* in our study (Table S3). However, no studies to our knowledge have commented on relationships between time of year and likelihood of specific temperature patterns, except to identify that such behaviours are more likely to occur in the summer as opposed to cooler times of the year. Though we did not include a predictor describing air temperature within our analysis, we indirectly accounted for seasonal and diel variations in solar radiation, which in turn drives air temperature and stream temperature, using two metrics, *date* and *ToD*. Thus, our findings are also in alignment with Somers et al. (2016), who found that heat pulse magnitude was somewhat correlated with the air temperature preceding the event. Air temperature is likely to be a key predictor of heat pulse magnitude; however, as our analysis relied on publicly available datasets, we do not have observations of air temperature at each of our sites. Given that air temperatures vary widely within urban areas, we opted to use these static predictors instead of observations of air temperatures, as it was not possible for us to guarantee these observations from other locations would be representative of behaviour at our particular site.

5.1 | Importance of site versus event characteristics

The initial analysis of the relative frequency of different event types revealed that a wide variety of event types occurred at most sites (Figure 2a), and only two sites showed a clear preference for a temperature increase over the other two general stream temperature patterns. This suggests that the general type of stream temperature response is more strongly linked to event characteristics than site characteristics.

When it comes to the type of temperature increase, however, individual sites appeared to display a clear preference for specific patterns (Figure 2b), either exhibiting a very rapid increase in stream temperature at the start of the event (a 'heat pulse'), or a much more gradual, delayed temperature increase. This preference for specific responses was consistent across the 3 years of data analysed here. An analysis of the importance of site characteristics, however, is beyond the scope of this paper, which focuses more specifically on response across events. It thus remains to be seen whether such patterns would hold at broad scales, which would require a comparison of a

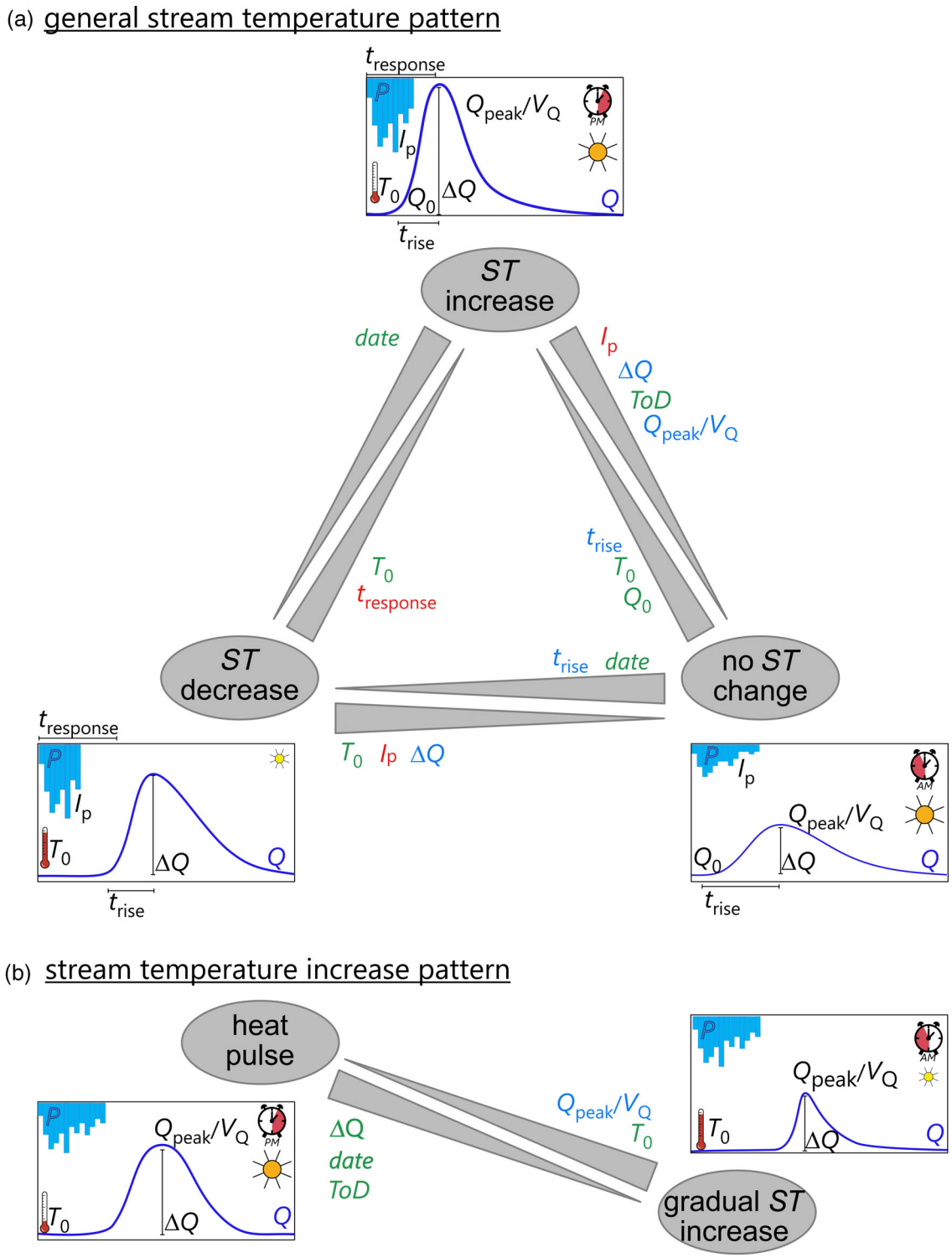

FIGURE 4 Illustration of the results of the logistic regression analyses for (a) the general temperature change pattern, and (b) the temperature increase pattern. The figure illustrates the relevant explanatory variables identified for each pattern, and the type of event characteristics most strongly associated with each temperature pattern. Predictor variables are coloured to indicate the characteristic types outlined in Table 2. The variable *ToD* is represented by a small clock (with AM and PM distinguishing between 'early in the day' and 'late in the day'), and the variable *date* by a sun (small yellow sun indicating early in the year and a large orange sun indicating later in the year).

substantially larger number of sites than the six investigated here. While other studies have investigated how site characteristics, such as shading, stream width, and drainage area, are related to temperature changes (Nelson & Palmer, 2007; Somers et al., 2013; Wissler et al., 2022; Zahn et al., 2021), our study uniquely links these behaviours to event characteristics and identified hydrograph metrics

(e.g., Q_{peak}/V_Q, ΔQ) as important predictors for the temperature patterns (Figures 3 and 4).

Nevertheless, the dominance of specific temperature patterns at some sites suggests that the response pattern may at least in part be site specific. In consequence, stream temperature patterns likely depend at least partially on local site characteristics, reflecting interactions between local climate, watershed and reach characteristics, and local weather conditions. As the literature most commonly attributes heat pulses to warm runoff from storm sewers (with potential for combined sewer overflows to also play a role), information on the presence of stormwater and combined sewer overflow locations would also be of interest when considering site specific patterns.

While our data should not be used to interpret the importance of land cover for specific temperature patterns, our findings do point to the relevance of landscape architecture and land cover at the local scale. In spite of the (semi-)urban character of all sites analysed here, the sites differ substantially with respect to the spatial distribution of forested and impervious areas within the watershed. For instance, while some watersheds contain forested buffer strips (of varied length and width) along the stream, others have a larger, continuous area with forest cover away from the channel or in the upstream area. A wealth of literature has spoken to the value of forested buffers for stream temperature (Hewlett & Fortson, 1982; Moore et al., 2005; Somers et al., 2013; Sweeney & Newbold, 2014), and previous work has shown that the location of imperviousness will influence streamflow response (Roodsari & Chandler, 2017). The local-scale land cover is thus likely to have an important effect on short-term stream temperature responses during storm events.

5.2 | Comparison of bootstrap and logistic regression results

The results of the bootstrap and logistic regression analyses are generally comparable and both analyses identify similar predictor variables that show a link between stream temperature response and hydrologic behaviour. For example, t_{rise}, I_p, and Q_{peak}/V_Q, were found to be important for distinguishing general stream temperature patterns in both analyses. In addition, the initial water temperature (T_0) was also a key explanatory variable for both types of analyses. However, the logistic regression analysis provides more detail on the relevance and direction of the parameters for specific stream temperature patterns compared to the bootstrap forest analysis.

Nevertheless, some results of the two analyses differ. For example, the result of the logistic regression analysis identifies $t_{response}$, *date* and ΔQ as relevant parameters for the general stream temperature patterns, while their relevance is deemed low based on the bootstrap forest outcomes. This may in part be due to a correlation of these parameters with other highly relevant characteristics (e.g., ΔQ is highly correlated with Q_{peak}/V_Q and I_p, which are identified in both analyses, and *date* and $t_{response}$ are correlated with T_0 and Q_0, which are again identified as relevant in various analysis aspects). Thus, their explanatory power is similar in the bootstrap forest analysis and one variable can be replaced by the other.

Importantly, we emphasize that, across these sites, we cannot link any of the observed patterns to only one or two specific predictor variables. Instead, a number of predictors together—characterizing several aspects of the storm event—determine the type of observed temperature response. This is illustrated by the largely overlapping ranges of the violin plots in Figure S10, which demonstrate that different patterns are simply *more likely* to occur within a given predictor range, but that the resulting pattern is determined by several predictors in concert.

5.3 | Stream temperature patterns and water release processes

Our analysis identified distinct stream temperature responses to storm events, and we were able to link these patterns to event characteristics (Figure 4). This indicates that water release processes are important drivers of stream temperature response patterns. Urban infrastructure is typically designed to rapidly route water to the sewer network to avoid flooding, and it appears logical that specific stream temperature responses may be related to event- and site-specific water sources contributing to streamflow. No changes in stream temperature are observed in the case of a slow rise in the hydrograph following a low-intensity precipitation event (Figure 4a), that is, these discharge increases may be caused by the slow seeping of soil water or groundwater into the channel at a rate that is too slow to substantially or quickly change the stream temperature. Stream temperature increases, on the other hand, are observed during events with quick and substantial discharge increases causing narrow and peaked hydrographs (Figure 4a), indicating that substantial amounts of surface runoff or water from the shallow subsurface are translated to the stream within a short amount of time. Finally, decreases in stream temperature are observed if response times between the precipitation input and hydrograph response are long and the pre-event stream temperature is high (Figure 4a). This pattern potentially implies the translation of larger amounts of water from upstream areas toward the gauge, though confirming the processes that generate such behaviour would require further monitoring and potentially stream temperature modelling. Similarly, the presence and absence of heat pulses seems to be linked to event characteristics, especially those describing the shape of the hydrograph (Figure 4b). This is particularly striking, since the heat pulse typically occurs very early and usually before any substantial change in flow has occurred, indicating that specific water release processes may trigger both a specific hydrograph shape as well as a heat pulse response.

The strong link between event characteristics and temperature patterns indicates the potential for stream temperature as inexpensive tracers for water sources and pathways in urban systems. However, further research is needed to disentangle the various empirical relationships and reveal potential physical controls on how (warm) water is conveyed to streams in urban systems.

5.4 | Prevalence and magnitude of heat pulses

Heat pulses represent a specific type of stream temperature increase, with a rapid rise in stream temperature at the very start of the storm event, followed by a subsequent temperature drop usually occurring before peak runoff is reached (Figure 1b). Given that heat pulses typically occur at the very start of an event, at a time when the discharge increase is yet marginal, the added runoff must be quite warm to create such a strong temperature increase. To estimate the temperature of this added runoff, we performed a simple mixing analysis for the events in 2019 with heat pulses at Carrol Creek (11 events between May 3 and August 28), Cobbs Creek (10 events between May 28 and September 4), and Little Stone Mountain Creek (4 events between June 11 and July 17). This mixing analysis showed that the added water during a heat pulse had an average temperature of around 24°C (assuming no change in baseflow contribution) with a range from 19.5 to 31.0°C at Carroll Creek, 19.3 to 27.8°C at Cobbs Creek, and 22.7 to 26.7°C at Little Stone Mountain Creek (Section S6 in the Supporting Information). The highest of these temperatures were calculated for events in July, August, and early September, when air temperature was likely very warm. Based on the calculated temperature of these added water contributions, we can pose some possible hypotheses regarding their origin that could be tested via field observations. First, we point out that these temperatures are likely too warm to indicate groundwater contributions or direct routing of same-event precipitation to the stream. When considering possible sources, all sources of water to the stream should be considered, including point sources (e.g., storm sewers and other sources of effluent) and diffuse sources that supply water to the stream. As observed in other studies, in many cases heat pulses are observed to be generated by contributions from storm sewers, as was observed by Somers et al. (2013) and Hester and Bauman (2013). Alternatively, heat pulses may result from contributions of runoff or water ponded on near-stream impervious surfaces (though most cities work to eliminate such areas) that has been heated by hot pavement (Omidvar et al., 2018), stormwater management ponds or detention basins (Sabouri et al., 2016), or wastewater treatment plants (e.g., Beganskas & Toran, 2021). It also remains unclear whether warmer water in the shallow subsurface that has been heated in the lead up to the event and entering the stream with the first flush of precipitation, could also contribute to these responses. However, further research is needed to identify the exact water sources of these contributions, and crucially, whether such mechanisms may differ across sites.

6 | CONCLUSIONS

In this study we analysed the stream temperature response during 403 storm events across three summers and six (semi-)urban catchments. Our results illustrate that stream temperature responses to discharge increases during storm events can be varied and range from temperature decreases to temperature increases. The type of response is substantially influenced by storm event characteristics, in particular characteristics of the hydrograph and of precipitation, whereas pre-event conditions appear to be less relevant. We also demonstrate that different sites are prone to specific types of stream temperature increase patterns, typically either featuring a rapid heat pulse at the start of the event, or a much more gradual temperature increase with a delay relative to the hydrograph increase.

The dependence of stream temperature responses to event characteristics indicates that different temperature patterns may be caused by different sources of water contributing to streamflow during storm events. The mixing of sources, and the timing of this mixing process, likely causes a unique stream temperature pattern. Even though we can speculate about the origin of the water sources contributing to streamflow based on the identified relationships, the exact processes remain uncertain. Further experimental data and numerical modelling are needed to disentangle these different contributions and their spatial origin in the catchment. However, if successful, this would enable the use of stream temperature as an inexpensive but effective tracer of water sources and pathways in urban systems, which are typically difficult to assess (Oswald et al., 2023).

Understanding sources and their likely impact on stream temperature is also important from a perspective of water quality and biogeochemical functioning. As shown here, shorter hydrograph rise times are linked to stream temperature increases during storm events. However, causal mechanisms linking urbanization, increasing fraction of impervious surfaces, pathways of water in urban catchments, and the occurrence and magnitude of heat pulses are still under explored. Further clarifying such links is not only important in the context of land cover change, but also when considering impacts from changing climate, which itself will likely lead to increases in air and water temperatures in the next century and further threaten ecosystem functioning.

FUNDING INFORMATION

None.

CONFLICT OF INTEREST STATEMENT

The authors declare that they have no conflict of interest.

DATA AVAILABILITY STATEMENT

All data used in this study are freely available from the USGS through the National Water Dashboard (https://dashboard.waterdata.usgs.gov).

ORCID

Julia L. A. Knapp https://orcid.org/0000-0003-0885-7829
Christa Kelleher https://orcid.org/0000-0003-3557-201X

REFERENCES

Arnell, N. W. (1998). Climate change and water resources in Britain. *Climatic Change*, *39*(1), 83–110. https://doi.org/10.1023/A:1005339412565

Arora, R., Toffolon, M., Tockner, K., & Venohr, M. (2018). Thermal discontinuities along a lowland river: The importance of urban areas and lakes. *Journal of Hydrology*, *564*, 811–823. https://doi.org/10.1016/J.JHYDROL.2018.05.066

Beganskas, S., & Toran, L. (2021). Urban stream temperature patterns: Spatial and temporal heterogeneity in the Philadelphia region,

Pennsylvania, USA. *Hydrological Processes*, *35*(2), e14039. https://doi.org/10.1002/HYP.14039

Dewitz, J. (2023). *National Land Cover Database (NLCD) 2021 products: U.S. Geological Survey Data Release*. https://doi.org/10.5066/P9JZ7AO3

DOE. (2022). *Hickey run watershed | ddoe*. https://doee.dc.gov/service/hickeyrun

Ehalt MacEdo, H., Lehner, B., Nicell, J., Grill, G., Li, J., Limtong, A., & Shakya, R. (2022). Distribution and characteristics of wastewater treatment plants within the global river network. *Earth System Science Data*, *14*(2), 559–577. https://doi.org/10.5194/ESSD-14-559-2022

Fanelli, R. M., Prestegaard, K. L., & Palmer, M. A. (2019). *Urban legacies: Aquatic stressors and low aquatic biodiversity persist despite implementation of regenerative stormwater conveyance systems*. https://doi.org/10.1086/706072

Gooseff, M. N., Strzepek, K., & Chapra, S. C. (2005). Modeling the potential effects of climate change on water temperature downstream of a shallow reservoir, lower Madison river, MT. *Climatic Change*, *68*(3), 331–353. https://doi.org/10.1007/S10584-005-9076-0

Hastie, T., Tibshirani, R., & Friedman, J. H. (2009). *The elements of statistical learning: Data mining, inference, and prediction. Springer series in statistics* (Vol. 27). Springer.

Hester, E. T., & Bauman, K. S. (2013). Stream and retention pond thermal response to heated summer runoff from urban impervious surfaces. *JAWRA Journal of the American Water Resources Association*, *49*(2), 328–342. https://doi.org/10.1111/JAWR.12019

Hewlett, J. D., & Fortson, J. C. (1982). Stream temperature under an inadequate buffer strip in the southeast Piedemont. *JAWRA Journal of the American Water Resources Association*, *18*(6), 983–988. https://doi.org/10.1111/J.1752-1688.1982.TB00105.X

Moore, R. D., Spittlehouse, D. L., & Story, A. (2005). Riparian microclimate and stream temperature response to forest harvesting: A review. *JAWRA Journal of the American Water Resources Association*, *41*(4), 813–834. https://doi.org/10.1111/J.1752-1688.2005.TB03772.X

Nelson, K. C., & Palmer, M. A. (2007). Stream temperature surges under urbanization and climate change: Data, models, and responses. *JAWRA Journal of the American Water Resources Association*, *43*(2), 440–452. https://doi.org/10.1111/J.1752-1688.2007.00034.X

Omidvar, H., Song, J., Yang, J., Arwatz, G., Wang, Z. H., Hultmark, M., Kaloush, K., & Bou-Zeid, E. (2018). Rapid modification of urban land surface temperature during rainfall. *Water Resources Research*, *54*(7), 4245–4264. https://doi.org/10.1029/2017WR022241

Oswald, C. J., Kelleher, C., Ledford, S. H., Hopkins, K. G., Sytsma, A., Tetzlaff, D., Toran, L., & Voter, C. (2023). Integrating urban water fluxes and moving beyond impervious surface cover: A review. *Journal of Hydrology*, *618*, 129188. https://doi.org/10.1016/J.JHYDROL.2023.129188

Ouellet, V., Khamis, K., Croghan, D., Hernandez Gonzalez, L. M., Rivera, V. A., Phillips, C. B., Packman, A. I., Miller, W. M., Hawke, R. G., Hannah, D. M., & Krause, S. (2021). Green roof vegetation management alters potential for water quality and temperature mitigation. *Ecohydrology*, *14*(6), e2321. https://doi.org/10.1002/ECO.2321

Paliwal, K. K., Agarwal, A., & Sinha, S. S. (1982). A modification over Sakoe and Chiba's dynamic time warping algorithm for isolated word recognition. *Signal Processing*, *4*(4), 329–333. https://doi.org/10.1016/0165-1684(82)90009-3

Roodsari, B. K., & Chandler, D. G. (2017). Distribution of surface imperviousness in small urban catchments predicts runoff peak flows and stream flashiness. *Hydrological Processes*, *31*(17), 2990–3002. https://doi.org/10.1002/HYP.11230

Sabouri, F., Gharabaghi, B., Sattar, A. M. A., & Thompson, A. M. (2016). Event-based stormwater management pond runoff temperature model. *Journal of Hydrology*, *540*, 306–316. https://doi.org/10.1016/J.JHYDROL.2016.06.017

Sakoe, H., & Chiba, S. (1978). Dynamic programming algorithm optimization for spoken word recognition. *IEEE Transactions on Acoustics, Speech, and Signal Processing*, *26*(1), 43–49. https://doi.org/10.1109/TASSP.1978.1163055

Somers, K. A., Bernhardt, E. S., Grace, J. B., Hassett, B. A., Sudduth, E. B., Wang, S., & Urban, D. L. (2013). Streams in the urban heat island: Spatial and temporal variability in temperature. *Freshwater Science*, *32*(1), 309–326. https://doi.org/10.1899/12-046.1/ASSET/IMAGES/LARGE/I2161-9565-32-1-309-F08.JPEG

Somers, K. A., Bernhardt, E. S., Mcglynn, B. L., & Urban, D. L. (2016). Downstream dissipation of storm flow heat pulses: A case study and its landscape-level implications. *JAWRA Journal of the American Water Resources Association*, *52*(2), 281–297. https://doi.org/10.1111/1752-1688.12382

Sweeney, B. W., & Newbold, J. D. (2014). Streamside forest buffer width needed to protect stream water quality, habitat, and organisms: A literature review. *JAWRA Journal of the American Water Resources Association*, *50*(3), 560–584. https://doi.org/10.1111/JAWR.12203

Tang, W., & Carey, S. K. (2017). HydRun: A MATLAB toolbox for rainfall–runoff analysis. *Hydrological Processes*, *31*(15), 2670–2682. https://doi.org/10.1002/HYP.11185

Timm, A., Ouellet, V., & Daniels, M. (2020). Swimming through the urban heat island: Can thermal mitigation practices reduce the stress? *River Research and Applications*, *36*(10), 1973–1984. https://doi.org/10.1002/RRA.3732

Timm, A., Ouellet, V., & Daniels, M. (2021). Riparian land cover, water temperature variability, and thermal stress for aquatic species in urban streams. *Water*, *13*(19), 2732. https://doi.org/10.3390/W13192732

Walsh, C. J., Roy, A. H., Feminella, J. W., Cottingham, P. D., Groffman, P. M., & Morgan, R. P. (2015). The urban stream syndrome: current knowledge and the search for a cure. *Journal of the North American Benthological Society*, *24*(3), 706–723. https://doi.org/10.1899/04-028.1

Winterbottom, J. H., Orton, S. E., & Hildrew, A. G. (1997). Field experiments on the mobility of benthic invertebrates in a southern English stream. *Freshwater Biology*, *38*(1), 37–47. https://doi.org/10.1046/J.1365-2427.1997.00191.X

Wissler, A. D., Segura, C., & Bladon, K. D. (2022). Comparing headwater stream thermal sensitivity across two distinct regions in Northern California. *Hydrological Processes*, *36*(3), e14517. https://doi.org/10.1002/HYP.14517

Zahn, E., Welty, C., Smith, J. A., Kemp, S. J., Baeck, M. L., & Bou-Zeid, E. (2021). The hydrological urban heat island: Determinants of acute and chronic heat stress in urban streams. *JAWRA Journal of the American Water Resources Association*, *57*(6), 941–955. https://doi.org/10.1111/1752-1688.12963

SUPPORTING INFORMATION

Additional supporting information can be found online in the Supporting Information section at the end of this article.

How to cite this article: Knapp, J. L. A., & Kelleher, C. (2023). The heat is on: Predicting urban stream temperature responses to summer storms. *Hydrological Processes*, *37*(11), e15033. https://doi.org/10.1002/hyp.15033